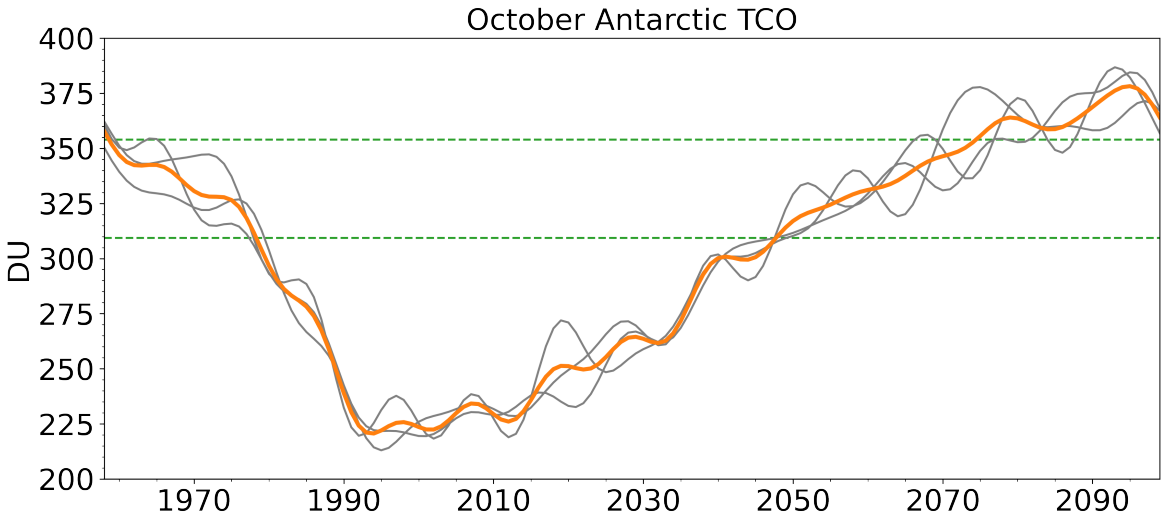

Figure S1. Ozone recovery in FOCI: time series of polar cap (60°S-90°S) total column ozone for October (DU). The INTERACT_O_3 ensemble mean is shown in orange and the individual members in gray. The horizontal green lines mark the 1980 and 1960 ozone levels, computed from the ensemble mean given as the 1979-1981 and 1959-1961 averages, respectively. The time series were filtered using a 10-point boxcar filter.

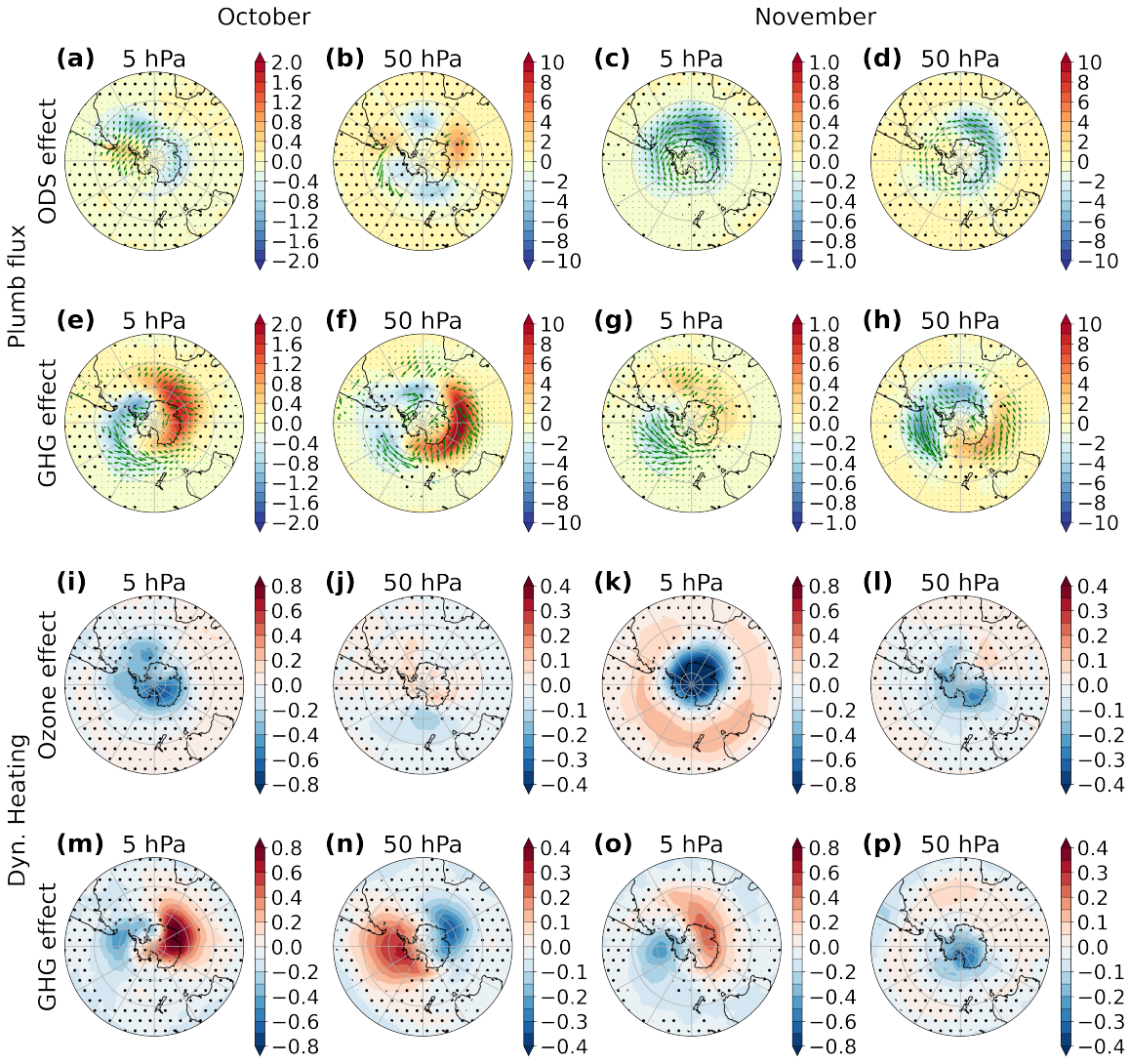

Figure S2. Changes in the flux of wave activity (a-h) and in the dynamical heating rate (i-p; K day^{-1}) at 50 hPa (b, d, f, h, j, l, n and p) and 5 hPa (a, c, e, g, i, k, m and o) during October (a, b, e, f, i, j, m and n) and November (c, d, g, h, k, l, o and p) due to ozone recovery (a-d and i-l) and increasing GHGs (e-h and m-p). The color shading in a-h shows the change in the vertical (10^{-3} m^2 s^{-2}) and the vectors show the change in the horizontal (m^2 s^{-2}) component of the flux. The stippling masks regions where the changes are not significant at the 95% confidence interval based on a two-tailed t-test.

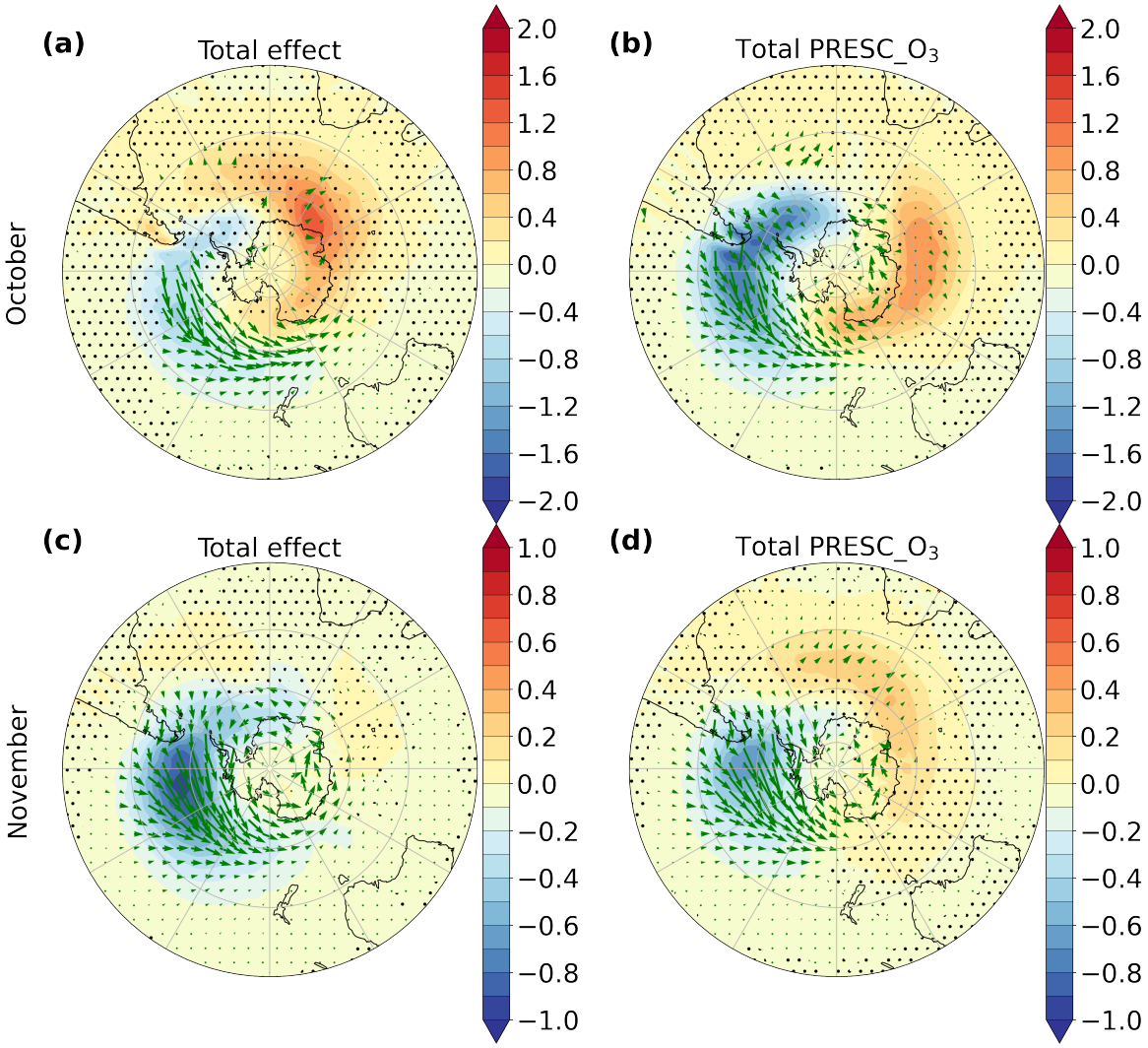

Figure S3. Changes in the flux of wave activity at 5 hPa during October (a and b) and November (c and d) due to ozone recovery and increasing GHGs combined, in INTERACT_O_3 (a and c) and PRESC_O_3 (b and d). The color shading shows the change in the vertical (10^{-3} $\mathrm{m^2\ s^{-2}}$) and the vectors show the change in the horizontal ($\mathrm{m^2\ s^{-2}}$) component of the flux. The stippling masks regions where the changes are not significant at the 95% confidence interval based on a two-tailed t-test.

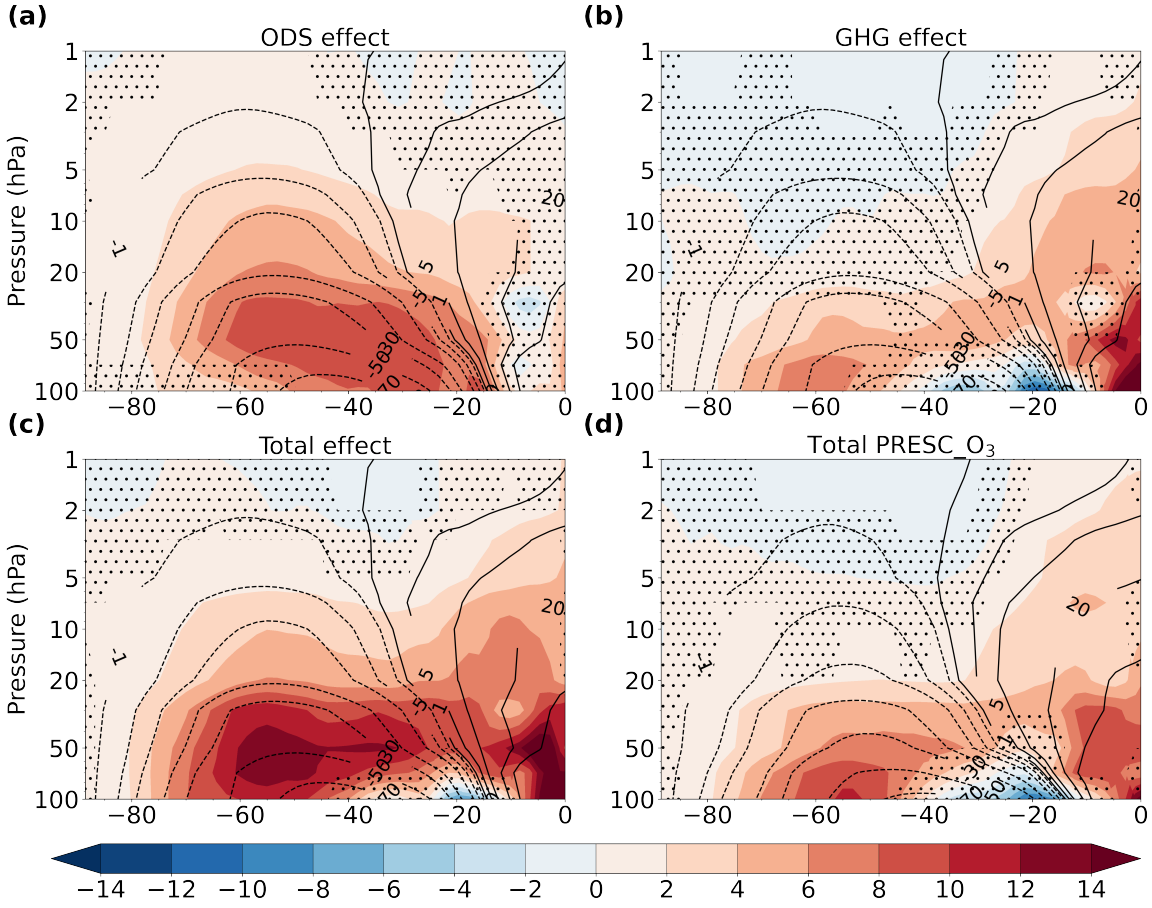

Figure S4. Changes in the mean residual streamfunction (kg m^{-1} s^{-1}) during November for each latitude and pressure level (color shading): effect of ozone recovery (a), effect of GHGs (b), total effect in INTERACT_O_3 (c) and total effect PRESC_O_3 (d). The contours depict the current day (2011-2030) November climatology from INTERACT_O_3 in a-c and from PRESC_O_3 in d. The stippling masks regions where the changes are not significant at the 95% confidence interval based on a two-tailed t-test.

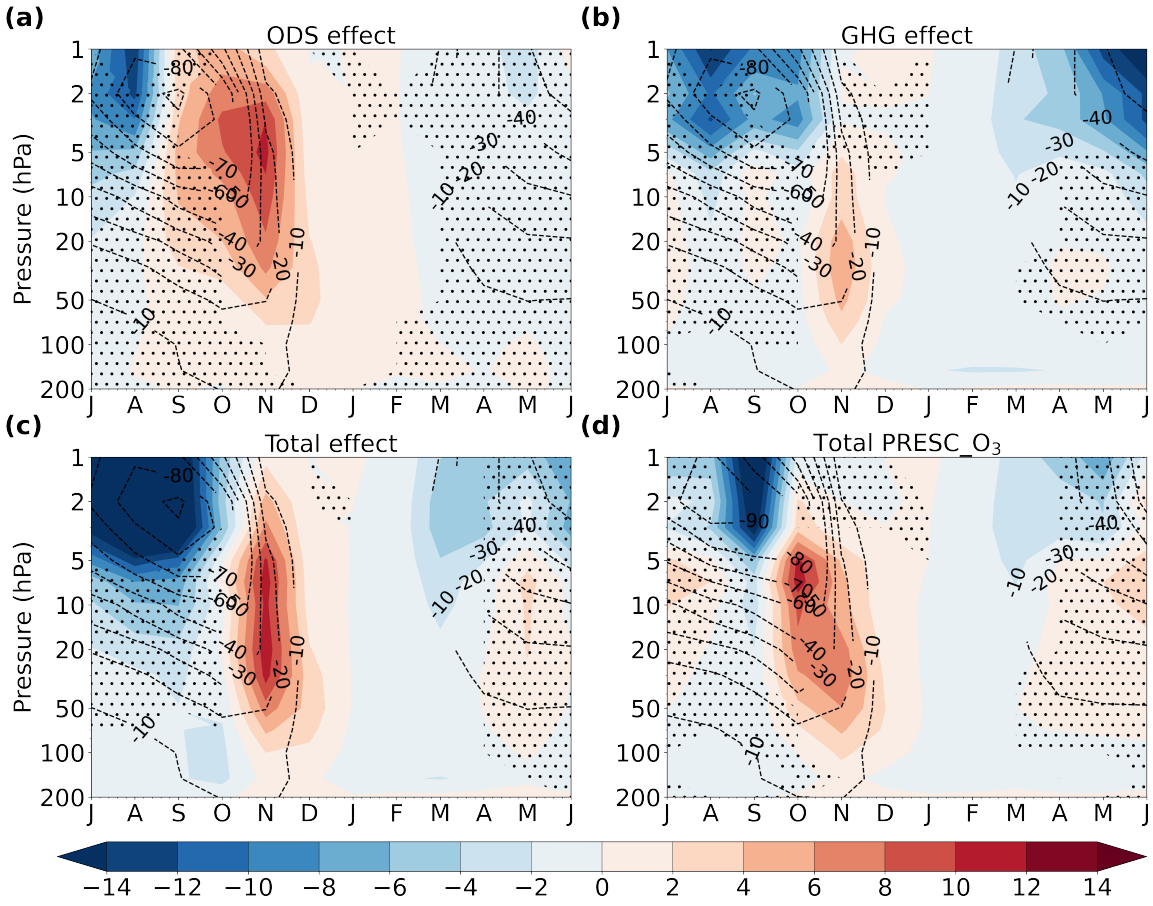

Figure S5. Changes in the eddy heat flux averaged over 45°S-80°S (kg m s^{-2}) for each month and pressure level (color shading): effect of ozone recovery (a), effect of GHGs (b), total effect in INTERACT_O_3 (c) and total effect in PRESC_O_3 (d). The contours depict the current day (2011-2030) climatology from INTERACT_O_3 in a-c and from PRESC_O_3 in d. The stippling masks regions where the changes are not significant at the 95% confidence interval based on a two-tailed t-test.

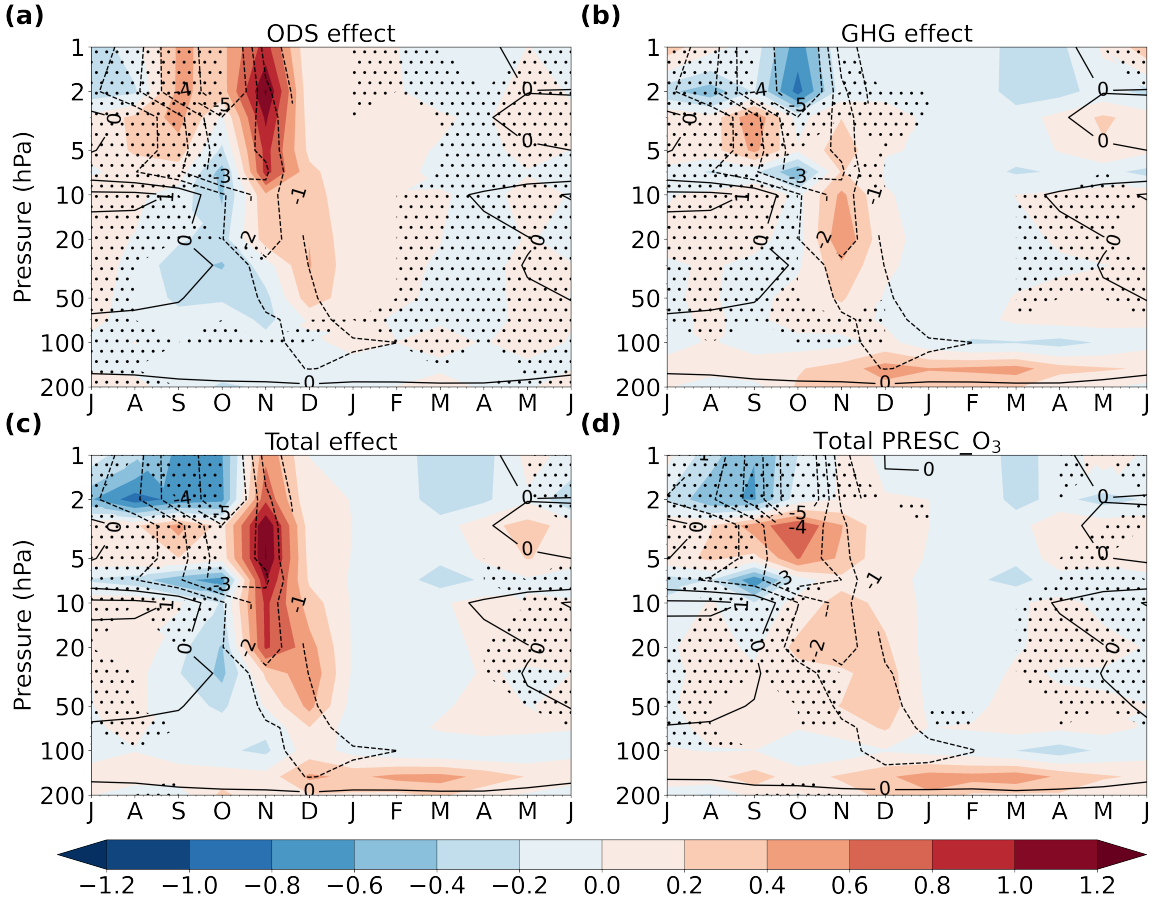

Figure S6. Changes in the divergence of the EP flux averaged over 45°S-80°S ($\mathrm{m\ s^{-1}\ day^{-1}}$) for each month and pressure level (color shading): effect of ozone recovery (a), effect of GHGs (b), total effect in INTERACT_O_3 (c) and total effect in PRESC_O_3 (d). The contours depict the current day (2011-2030) climatology from INTERACT_O_3 in a-c and from PRESC_O_3 in d. The stippling masks regions where the changes are not significant at the 95% confidence interval based on a two-tailed t-test.

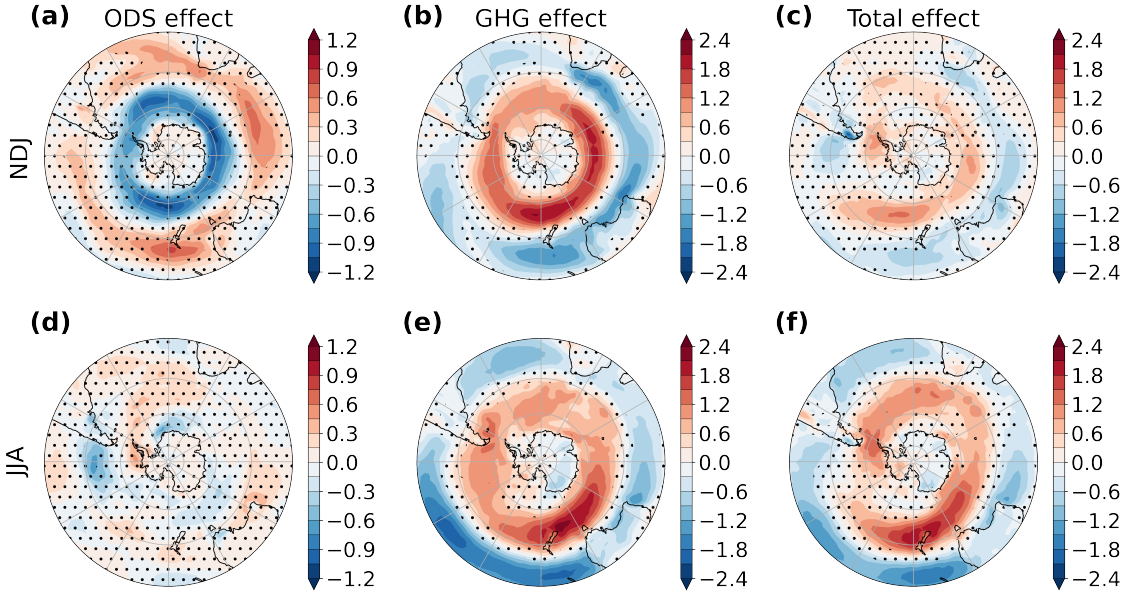

Figure S7. Changes in the surface zonal wind ($\mathrm{m\ s^{-1}}$) during November-January (a-c) and June-August (d-f) due to ozone recovery (a and d), GHGs (b and e) and their combined effect in INTERACT_O_3 (c and f). The stippling masks regions where the changes are not significant at the 95% confidence interval based on a two-tailed t-test.